RSC Advances

ROYAL SOCIETY OF CHEMISTRY

www.rsc.org/advances

Increased sensitivity of extracellular glucose monitoring based on AuNP decorated GO nanocomposites

Qi Meng,[a] *Yin Zhang,*[a] *Chaomin Cao,*[a] *Yang Lu,*[c] *Guozhen Liu,*[a, b]*

[a]Key Laboratory of Pesticide and Chemical Biology of Ministry of Education, College of Chemistry, Central China Normal University, Wuhan 430079, P. R. China

[b]ARC Centre of Excellence in Nanoscale Biophotonics (CNBP), Department of Physics and Astronomy, Macquarie University, North Ryde 2109, Australia

[c]Key Laboratory of Food Nutrition and Safety, Ministry of Education of China, Tianjin University of Science and Technology, Tianjin, 300457, China

*To whom correspondence should be addressed. Email: gzliu@mail.ccnu.edu.cn. Tel: +86-27-6786 7535

ABSTRACT

AuNP decorated GO nanocomposites (GO-Ph-AuNP) via aryldiazonium salt chemistry have been successfully prepared, which can be used as the immobilization matrix for loading glucose oxidase (GOx) towards a sensitive glucose sensor. The fabricated nanocomposite was characterized by field emission scanning electron microscope, UV-Vis and electrochemistry. The direct electrochemistry of GOx was successfully realized on GO-Ph-AuNP modified GC electrodes with heterogeneous electron transfer rate constant of 8.3 s^{-1}, revealing a fast direct electron transfer of GOx. The GOx immobilized on GO-Ph-AuNP nanocomposite modified electrode

retained good electrocatalytic activity toward glucose over a linear concentration range from 0.3 to 20 mM with the sensitivity of 42 μA mM^{-1} cm^{-2} and enzyme turnover rate of 112 s^{-1}. Besides, the fabricated biosensor showed the capability of monitoring the glucose consumptions by live cells.

Keywords: Graphene oxides, gold nanoparticles, sensitivity, glucose monitoring

INTRODUCTION

The development of rapid, simple and reliable methods of monitoring glucose is important in many areas such as clinical diagnostics, medicine and food industry. Glucose metabolism not only is the main energy source for cells, but also provides essential biomass for proliferating cells, including cancer cells. Many diseases are associated with glucose transport and metabolic disorders, such as myocardial ischemia, type 2 diabetes and cancer.[1] Therefore, monitoring glucose metabolism of cells can provide important information that reflects cell responses to stimuli and proliferative states, which are extremely useful to cancer therapeutic diagnoses, wound healing diagnoses and for fundamental understating of biological processes of the metabolism.[2] Ever since Clark and Lyons[3] introduced the first enzyme sensor employing glucose oxidase (GOx) and an oxygen electrode for glucose monitoring, innumerable glucose sensors and devices have been developed by researchers in this field, including electrochemical glucose sensors,[4] optical (fluorescence and absorbance) glucose sensors,[5] and boronic acid based glucose sensors.[6] GOx based enzyme electrodes have been widely used as the gold standard for glucose sensing due to their high sensitivity and selectivity.[7] Because native GOx is unable to transfer electrons to conventional electrode surfaces, the enzyme was inadequate for third-generation glucose sensors. Efforts have been focused on connecting the enzyme's redox center to the electrode by employing various molecular wires, such as rigid and conductive molecules,[8,9] osmium complex-linked polymers,[10] carbon based nanomaterials,[11,12] or nanofibers.[13] Alternatively, deglycosylating the enzyme

increased the efficiency of direct electron transfer ability,[14] presumably by decreasing the distance between the enzyme's redox center and the electrode. Among them, nanomaterial based glucose sensors are attractive due to the significantly enhance sensitivity.

Both of graphene based materials[15,16] and gold nanoparticles (AuNPs)[17] are the frequently used nanomaterials in the field of electrochemical biosensors due to their excellent electrical signal amplification and the versatile functionalization chemistry. For example, a highly sensitive and selective electrochemical dopamine sensor based on multilayer graphene nanobelts was developed with the sensitivity of 0.95 $\mu A\ \mu M^{-1}\ cm^{-2}$.[18] Recently, to incorporate advantages of both GO and AuNPs together, AuNPs decorated GO nanocomposites have received special interests for development of advanced materials for utilization in different fields[19,20] by providing strongly enhanced properties.[21] For example, a 3D GO-encapsulated AuNP, is developed to induce the double enhancement effect of GO and AuNP on surface-enhanced Raman spectroscopy signals, which provides a powerful non-destructive *in situ* monitoring tool for the identification of the differentiation potential of various kinds of stem cells.[22] The gold nanoparticle-decorated graphene oxides were used for polymer photovoltaic devices based on the enhanced plasmonic property.[23,24] The nonlinear absorption and refraction of the GO hybrid films were strongly enhanced by the presence of AuNP.[25] We have incorptated the AuNPs into GO sheets to achieve increased sensitivity for detection of cardiac marker troponin-I.[26] There are various methods for formation of AuNP/GO nanocomposites, such as electrostatic adsorption,[27] hydrophobic and π-π interaction,[28] S-Au bonding[29], and NH-Au bonding.[30] The most frequently used method is based on the reaction of gold trichloride with GO under reductive conditions for in situ anchoring AuNP to GO. This method, however, often lacked fine control over the size, the uniformity and the density of AuNP on the sheets in the reaction process. In addition, the stability of AuNP is compromised comparing to the binding of AuNP by Au-C binding.[31]

In this study, we prepared the AuNP loaded GO nanocomposites by Au-C bonding through in situ aryldiazonium salt chemistry. After that, the AuNP loaded GO

nanocomposites can be modified onto GC electrodes by C-C binding. Then 4-carboxyphenyl was modified onto AuNP by aryldiazonium salt chemistry, which was used for binding the GOx to achieve glucose sensing interface. The glucose sensor was used to monitor glucose changes during the growth and respiration processes of human umbilical vein endothelial cells (HUVECs) and human cervical cancer HeLa cell lines.

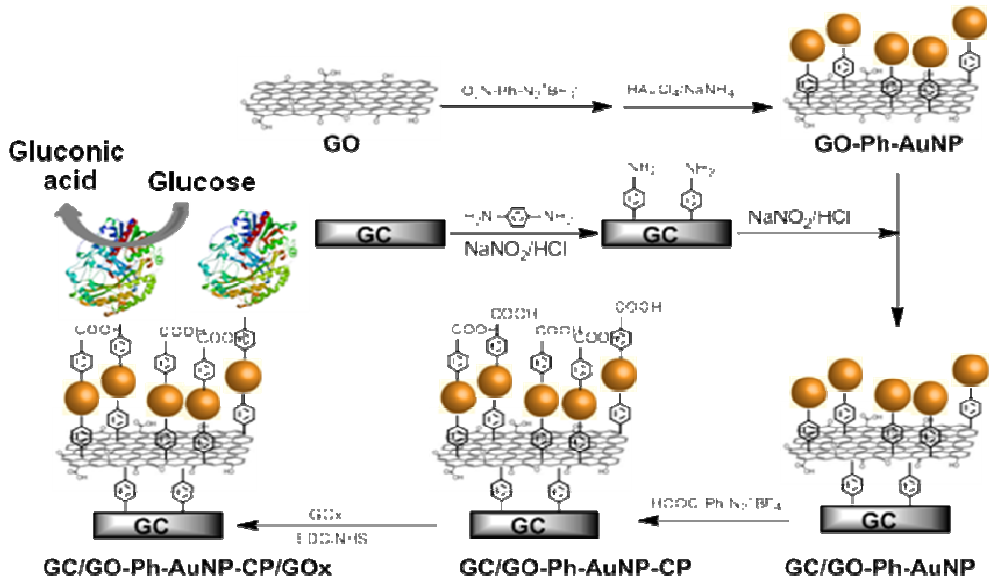

Scheme 1. The scheme of a glucose biosensor based on AuNP loaded GO nanocomposites (GO-Ph-AuNP). Based on aryldiazonium salt chemistry, AuNPs were decorated to GO through a benzene bridging. GO-Ph-AuNP was then attached to the 4-aminophenyl modified GC electrode by C-C bonding. The formed GC/GO-Ph-AuNP interface was further modified with 4-carboxyphenyl before covalent attachment of glucose oxides (GOx) by amide bonds to achieve the GC/GO-Ph-AuNP-CP/GOx sensing interface.

EXPERIMENTAL SECTION

Chemicals and Instruments

Graphene oxide, hydrochloric acid, sulfuric acid, absolute ethanol, potassium chloride, gold trichloride, potassium ferricyanide, ferrocene, trifluoroacetic anhydride, tris(hydroxymethyl)aminomethane (Tris), sodium nitrite, sodium cyanoborohydride,

acetonitrile (CH_3CN, HPLC grade), 1-ethyl-3-(3-dimethylaminopropyl)carbodiimide hydrochloride (EDC), N-hydroxysuccinimide (NHS), glucose oxides, and 4-nitrophenyl diazonium tetrafluoroborate were purchased from Sigma-Aldrich. The 4-carboxyphenyl were custom synthesized as reported previously.[32] ferrocenemethylamine was synthesized using the procedure from Kraatz,[33] Phosphate buffer solution used in this work contained 0.05 M KCl and 0.05 M K_2HPO_4/KH_2PO_4 adjusted to pH 7.0 with NaOH or HCl solution. All electrochemical experiments were conducted CHI 660E potentiostat (CH Instruments, Inc., Shanghai). GC electrodes were 3 mm disks embedded in epoxy resin (GaossUnion, China). All experiments utilized a Pt secondary electrode and a SCE (3.0 M NaCl) reference electrode. Scanning electron microscopy (SEM) was carried out using a Hitachi S-900 SEM (Berkshire, England). Transmission Electron Microscope (TEM) studies were performed with a JEM-2100 (HR) instrument at a voltage of 200 kV. Uv-Vis absorption data were collected on a Shimadzu Uv-Vis spectrophotometer model 2450.

Preparation of GO-Ph-AuNPs nanocomposites

All glassware was cleaned with piranha (H_2SO_4/H_2O_2 3:1 v/v) followed by aqua regia (HCl/HNO_3 3:1 v/v), then rinsed with copious amounts of distilled water before nanoparticle synthesis and functionalization. The graphene oxides (3 mg) was dissolved in 3.0 mL ice-cold HCl solution containing 30 mM $NaNO_2$ and 30 mM 4-nitrophenyl diazonium salt. The mixture was stirred in ice bath for 2 h. Then the solution was washed three times by centrifugation, and the collected solid was finally dispersed in 1.0 mL water to get 4-nitrophenyl modified GO. Finally, the

4-nitrophenyl modified GO (1 mL) was mixed with 400 μL 10 mM $HAuCl_4$ aqueous solution followed by adding 1 mL $NaBH_4$ ice-cold water solution (24 mM) immediately. The mixture solution was stirred for 2 h at room temperature, washed three times by centrifugation, and the obtained solid was finally dispersed in water solution with the final volume of 1 mL to get the GO-Ph-AuNP nanocomposites.

Preparation of the sensing interface

Commercial GC electrodes (CHI, Shanghai) were hand-polished successively in 1.0, 0.3 and 0.05 μm alumina slurries made from dry alumina and water on microcloth pads (Buehler, Lake Bluff, IL, USA). The electrodes were thoroughly rinsed with water and sonicated in water for 1 min between polishing steps. Prior to derivatization with aryl diazonium salts, the electrode was dried under a stream of argon. Then 1 mM 4-phenylenediamine was dissolved in 0.5 M aqueous HCl, to which 1 mM $NaNO_2$ was added. The mixture was degassed with nitrogen flow and left to react in the electrochemical cell for about 10 min at 0 °C to generate in situ aryl diazonium salt (H_2N-Ph-$N_2^+Cl^-$). The electrochemical reductive modification of GC electrodes with H_2N-Ph-$N_2^+Cl^-$ was carried out by scanning in a potential range between 0.6 V and -1.0 V for two cycles at a scan rate of 100 mV s^{-1} versus SCE, which were then rinsed with copious amounts of Milli-Q water, acetonitrile, and Milli-Q water, respectively, and finally dried under a stream of nitrogen prior to the next step. Then GO-Ph-AuNPs nanocomposites were modified to GC-Ph-NH_2 surface through C-C coupling by fixing potential at 0.3 V for 300 s in the GO-Ph-AuNP nanocomposites solution (1 mg mL^{-1}) containing 5 mM $NaNO_2$ and 0.5 M HCl versus SCE to get the

GC/GO-Ph-AuNPs surfaces. Then GC/GO-Ph-AuNPs were subsequently soaked in the 40 mM EDC and 10 mM NHS in 0.1 M MES buffer for 30 min to activate the carboxylic acid group on AuNPs. GC/GO-Ph-AuNPs/Ab_c surfaces were obtained by incubation of activated GC/GO-Ph-AuNPs surfaces in Tris buffer pH 7.3 containing 1 mM glucose oxides for overnight at 4 ^{o}C (Scheme 1).

Cell culture for extracellular glucose monitoring

Cells were cultured in a T75 cm^2 flask containing Dulbecco's Modified Eagle's medium (DMEM) supplement with 10% FBS, 100 U mL^{-1} of penicillin, 0.1 $mg.mL^{-1}$ of streptomycin (Life Technologies, Australia). The flask was placed in a humidified atmosphere with 5% CO_2 at 37 ^{o}C in a cell culture incubator (Sanyo, Japan). The media was replaced once every two days. The cells were cultured to about 80-90% confluence before harvest. During harvest, the cells were washed twice with Dulbecco's phosphate buffer saline (DPBS) followed by trypsinization using 2 mL trypsin to detach the cells from the flask. The trypsin was neutralized by adding 4 mL of fresh supplemented medium, and the harvested cells in DMEM medium suspension was transferred into a centrifuge tube and centrifuged at 200 rcf for 6 min. The supernatant was discarded and the final cell pellet was re-suspended into fresh medium. The fabricated sensor interface was dipped into a 10 mL test tube containing 2 mL of cell culture media with 10 mM of glucose to get the required concentration for experiments. Time dependent amperometry was monitored.

RESULTS AND DISCUSSION

High resolution transmission electron microscope analysis of prepared GO-Ph-AuNP nanocomposites

The morphology and structure of GO-Ph-AuNP nanocomposites were investigated by high resolution transmission electron microscope (HRTEM). It is observed from Figure 1a that AuNPs are distributed on GO sheets with a well-dispersed high density of AuNPs. The size of AuNPs ranges from 2 to 15 nm. The HRTEM images of AuNPs embedded on GO nanosheets are shown in Figure 1c, and the measured fringe lattice of AuNPs corresponds to the (111) plane is found to be 0.23 nm (Inset Figure 1c). Figure 1d shows that the diffraction dots are resolved in the selected area of electron diffraction (SAED) images, implying the crystalline nature of the AuNPs on the GO nanosheets. The XRD pattern of GO shows two peaks at 2θ value of 10.1°and 20.6° which are the characteristic peaks of GO (Figure 1 e). For the pattern of GO-Ph-AuNP nanocomposites, in addition to the characteristic peaks of GO, there are another four prominent peaks at 2θ values of about 37.9°,43.9°,64.5°,76.9° which are assigned to the (111), (200), (220), (311) crystallographic planes of cubic AuNPs (JCPDS card No. 004-0784), respectively. Thus this result is consistent with the SAED pattern, and AuNPs were successfully loaded on GO. In addition, the high intense diffraction peak observed at 37.9°confirms that the nanoparticles are composed of pure crystalline Au.[34]

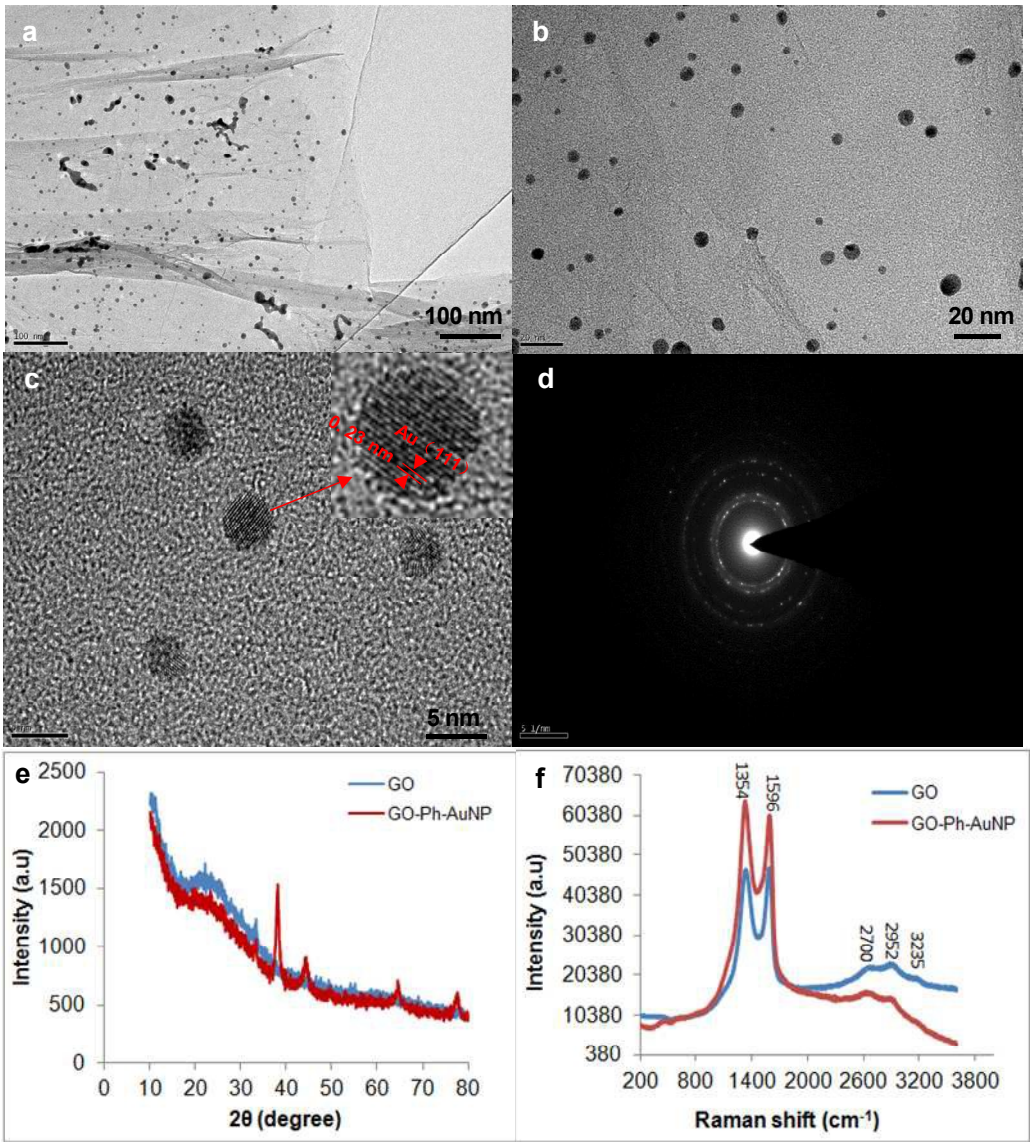

Figure 1. (a) Low-magnified HRTEM image of GO-Ph-AuNP nanocomposites. (b-c) HRTEM image of GO-Ph-AuNP nanocomposites in high magnifications (insert: with fringes of AuNPs along with interplanar spacing). (d) SAED image of AuNPs. (e) XRD spectrum of GO and GO-Ph-AuNP. (f) Ramam spectrum of GO and GO-Ph-AuNP.

Raman spectrum and UV-Vis spectroscopy for GO and GO-Ph-AuNP

Raman spectrums of GO and GO-Ph-AuNP are displayed in the Figure 1 f. The D and G peaks were observed at 1354 and 1596 cm^{-1}, respectively, in both the GO and GO-Ph-AuNP. The other three little peaks are derivatives of D- and G-band. D-band

is related to the disorder carbon structure induced by lattice defects and G-band is associated to well-ordered structure.[35] Therefore, the intensity ratio of D-band to G-band (I_D/I_G) can be used to present the graphitic character. As shown in the Figure 1 f the value of I_D/I_G of GO and GO-Ph-AuNP increased from 1.0374 to 1.0594, indicating that most of the oxygenated groups have been removed during the loading process.[34] The optical absorption spectra of the initial GO, AuNP (10 nm) colloid solution, and GO-Ph-AuNP nanocomposites are presented in Figure 2. Aqueous GO suspensions display a strong peak at ~300 nm due to n–π* transition of C=O bonds. For GO-Ph-AuNP nanocomposites suspensions in water, the absorption shifts to ~315 nm because of the removal of oxygen-containing bonds.[36] The plasmonic band of the Au nanostructure emerged at ~517 nm, corresponding to AuNPs of ~10 nm in size,[37] in accordance with TEM images.

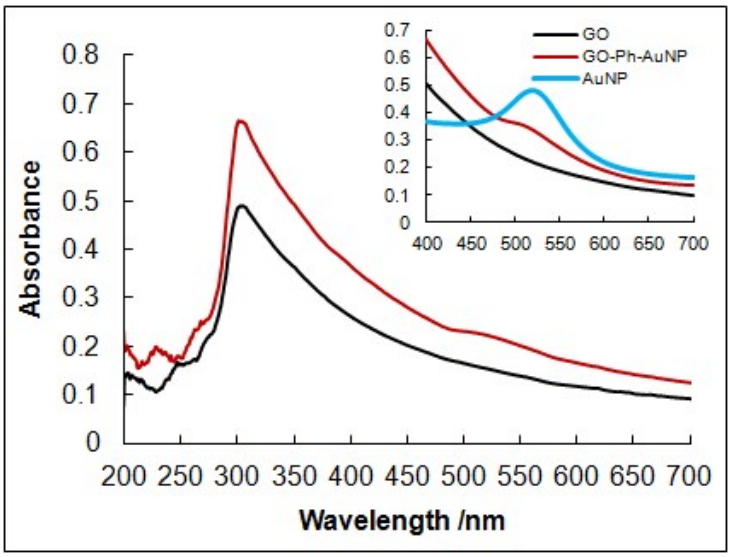

Figure 2. UV-vis absorption spectra of GO and GO-Ph-AuNPs suspensions (insert: UV-vis spectra for GO, AuNP and GO-Ph-AuNP nanocomposites.

Electrochemistry for GO-Ph-AuNP nanocomposites modified on GC electrodes

As shown in Scheme 1, GO-Ph-AuNP nanocomposites can be covalently modified to GC electrodes. Figure 3a shows the electrochemistry in 0.05 M H_2SO_4 for GC surfaces before and after the attachment of GO-Ph-AuNP. The appearance of a

reductive peak at about 0.8 V confirms the successfully attachment of AuNPs to the GC interface. Cyclic voltammetry was employed to investigate the electrochemistry of various modified GC electrodes in $Fe(CN)_6^{3-}/Fe(CN)_6^{4-}$ redox couple solution. Figure 3b shows the cyclic voltammograms of 4-aminphenyl modified GC, GC/GO-Ph-AuNP, GC/GO-Ph-AuNP-CP, GC/GO-Ph-AuNP-CP/GOx surfaces. Being different from the electrochemistry of a bare GC electrode in $Fe(CN)_6^{3-}/Fe(CN)_6^{4-}$ (a well-defined redox peaks centered at 0.2 V), the 4-aminphenyl modified GC surface resulted in prevention of access of the $Fe(CN)_6^{3-}/Fe(CN)_6^{4-}$ redox species to the electrode and hence no Faradaic peaks for ferricyanide were observed between -0.2 V to +0.6 V (Figure 3b solid line). An increase in the peak current of the redox couple was observed (Figure 3b dotted line) after the attachment of GO-Ph-AuNP nanocomposites. This increase in electron transfer rate upon attachment of GO-Ph-AuNP nanocomposites is consistent with previous observations which shows that AuNP loaded GO nanocomposites can increase the electronic coupling to the underlying electrode.[38] After modification of 4-carboxylphenyl species on AuNP surfaces, the peak current of the redox couple decreased, showing GC/GO-Ph-AuNP-CP surface (Figure 3b dashed line) restricted the access of $Fe(CN)_6^{3-}/Fe(CN)_6^{4-}$ redox probe to the AuNP surface due to the presence of 4-carboxylphenyl groups. With the further immobilization of GOx, the peak current of redox couple decreased significantly (Figure 3b dash dotted line), which indicates GOx has been successfully attached on the surfaces of GC/GO-Ph-AuNP-CP, thus covering the nanoparticles with protein and inhibiting access of the

$Fe(CN)_6^{3-}/Fe(CN)_6^{4-}$ redox couple to the electroactive elements on the surface.

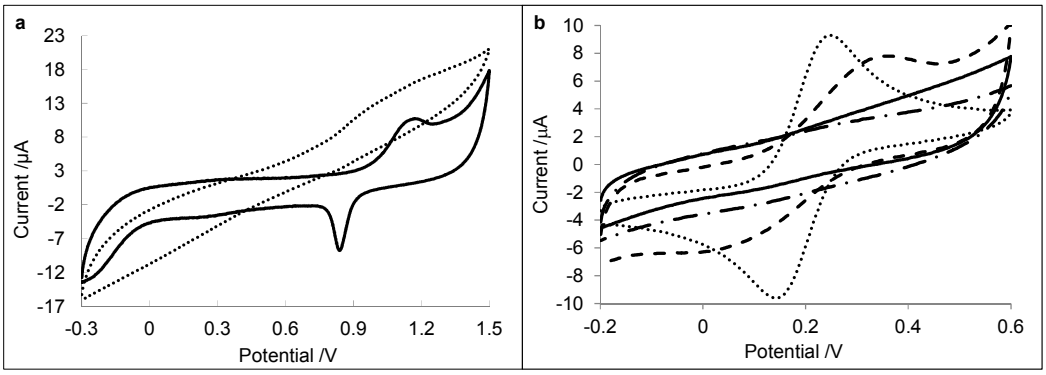

Figure 3. (a) CV of the GC surfaces before (dotted line) and after (solid line) attachment of GO-Ph-AuNP nanocomposites in 0.05 M H_2SO_4 at the scan rate of 100 mV s^{-1}. (b) CV recorded in phosphate buffer solution containing 0.05 M KCl and 1 mM $Fe(CN)_6^{3-}/Fe(CN)_6^{4-}$ with the scan rate of 100 mV s^{-1} for surfaces of 4-aminphenyl modified GC (solid line), GC/GO-Ph-AuNP (dotted line), GC/GO-Ph-AuNP-CP (dashed line), GC/GO-Ph-AuNP-CP/GOx (dash dotted line).

Electrochemistry of GOx Coupled on GC/GO-Ph-AuNP-CP surfaces

After incubation in 1 mM GOx solution for overnight at 4 ^oC, GC/GO-Ph-AuNP-CP surfaces showed reversible redox peaks of GOx in phosphate buffer (pH 7.0) in the absence of oxygen (Figure 4a solid line). In addition, a very stable voltammogram, without significant diminution of peak current after multiple scans, was obtained, suggesting that the GOx is tightly associated with the GC/GO-Ph-AuNP-CP interface. Controls show that GC electrodes modified with pure GO or pure AuNP gave no response in this potential range after incubation in the GOx solution under the same conditions. The formal potential ($E^{o`}$) for the GOx redox peaks in Figure 4a is about -481 mV (vs. SCE) with ΔE_p of 21 mV which is consistent with the reported formal

potential ($E^{o`}$=-422 mV vs. Ag/AgCl) for GOx modified on reduced graphene oxides and silver nanoparticle nanocomposite modified electrode.[39] The small ΔE_p demonstrates faster electron transfer between GOx and the modified electrode surface. The surface coverage of GOx was calculated to be 3.65×10^{-12} mol cm^{-2} was found for the 3 mm diameter circular GC electrodes, which is higher than that of GOx (2.41×10^{-12} mol cm^{-2}) on molecule wire modified GC electrodes.[40] This result proves that the large surface area of GO-Ph-AuNP nanocomposites facilitates the high enzyme loading. The cyclic voltammograms of the GOx incubated GC electrodes with different scan rates are shown in Figure 4b. The redox peaks showed linear variation in peak current with scan rates (Figure 4b insert), indicating that the adsorbed GOx performed as a surface-confined electrode reaction. The rate constant of electron transfer between redox centre of GOx and GC electrodes was calculated to be 8.3 s^{-1} using Laviron's method,[41] which is slightly higher than that of GOx on reduced graphene oxide and silver nanoparticles nanocomposite modified electrode.[39]

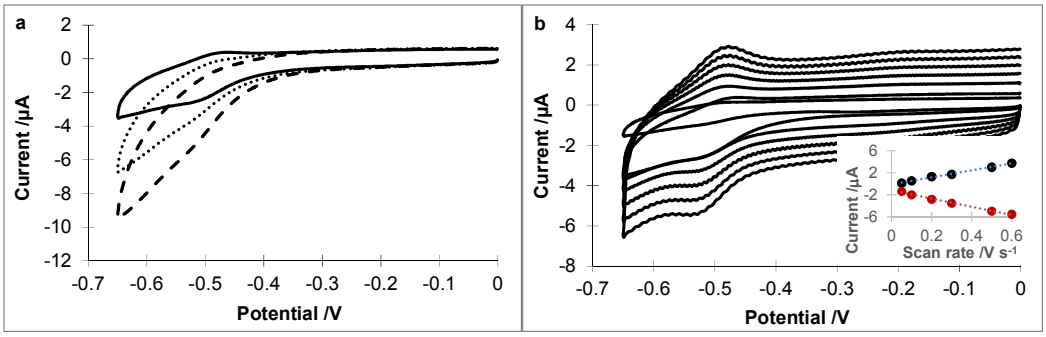

Figure 4. (a) Cyclic voltammograms of GC/GO-Ph-AuNP-CP electrodes in pH 7.0 phosphate buffer solution at the scan rate of 100 mV s^{-1} (solid line: in the absence of dissolved oxygen; dashed line: in the presence of dissolved oxygen with 0 mM glucose; dotted line: in the presence of dissolved oxygen with 10 mM glucose). (b)

Cyclic voltammograms of GC/GO-Ph-AuNP-CP electrodes in deoxygenated pH 7.0 phosphate buffer solution at scan rates of 50, 100, 200, 300, 400, 500 and 600 mV s^{-1} from inside cyclic voltammograms to outside cyclic voltammograms.

In order to explore glucose-specific enzyme activity of GOx modified on GC/GO-Ph-AuNP-CP surfaces, the electrochemistry of GOx was investigated under aerobic (in the presence of oxygen) and anaerobic (oxygen free) conditions (Figure 4a**).** After adding 10 mM glucose to the phosphate buffer solution saturated with oxygen, the cyclic voltammogram (Figure 4a dotted line) shifted up and reached close to the cyclic voltammogram under the oxygen-free condition without adding glucose. These results are consistent with the redox reaction of GOx in the presence of glucose under aerobic conditions. In the presence of glucose, the active centre FAD of GOx is reduced to $FADH_2$, and in the presence of oxygen, $FADH_2$ is oxidised to regenerate FAD and restore the catalytic form of GOx. Therefore in this process only the oxygen reduction was observed, resulting in the increase of the reduction peak current. So the results demonstrate that the molecular oxygen was consumed at the electrode surface and accordingly confirms that the GOx still maintained its specific enzyme activity and is sensitive to glucose. Thus the direct electron transfer between glucose and the GO-Ph-AuNP modified electrode efficiently generates an amperometric output signal (Scheme 1). The improved sensing performance by the direct electron transfer has been realized by incorporating the GOx with AuNPs resulting in the third generation glucose sensor. Owing to its highly specific surface area, good biocompatibility and stability, the gold nanoparticles on GO-Ph-AuNP act as an electrical nanoplug for

plugging into the redox active centre of GOx.[42]

Measurement of Biocatalytical Activity of GOx

The biocatalytical activity of GOx was also measured under anaerobic conditions (degassed with argon for 30 min before measurement) by injection of glucose at different concentrations. A chronoamperometry experiment at a constant potential of -430 mV that is close to the oxidation potential of GOx was carried out under constant stirring by adding glucose with different concentrations (Figure 5a). Upon the addition of glucose, the monitored current of GC/GO-Ph-AuNP-CP/GOx electrodes increased accordingly. However, no increase in oxidation current corresponding to the amount of glucose injected was observed at a GC/GO-Ph-AuNP-CP electrode, suggesting that the increase of oxidation current in Figure 5a is due to the redox reaction of GOx with glucose and is consistent with the biocatalytical reaction of GOx in the presence of glucose under anaerobic conditions. According to the biocatalytical reaction of GOx, in the presence of glucose GOx can catalyse glucose into gluconolactone and the native GOx-FAD becomes reduced to GOx-$FADH_2$. Under anaerobic (oxygen free) condition, the only way to recycle the reduced form of $FADH_2$ to FAD is *via* direct electron transfer, which is an oxidation process and will cause the increase of oxidation current correspondingly. Based on results of chronoamperometry experiments at a constant potential of -430 mV for GC/GO-Ph-AuNP-CP/GOx electrodes, the relationship between the current and the concentration of glucose is plotted in Figure 5b. The catalytic oxidation current in the absence of oxygen increased linearly with increasing glucose concentration and

saturated at glucose concentrations higher than 20 mM. Thus the sensitivity of the designed glucose sensor is 3.9 μA mM^{-1} cm^{-2}, which is lower than that of the recently reported glucose sensor based on reduced graphene oxide biocomposites (42 μA mM^{-1} cm^{-2}),[43] higher than that of GO modified glucose sensor (3 μA mM^{-1} cm^{-2}),[44] and similar to that of reduced GO and silver nanoparticles modified glucose sensor (3.84 μA mM^{-1} cm^{-2}).[37] The linear range of this sensor is 0.3-20 mM with the detection limit of 0.3 mM of glucose. From the known surface coverage of the enzyme (3.65 mol cm^{-2}) and the saturated current density (78.9 μA cm^{-2}), the enzyme turnover rate can be calculated to be 112 s^{-1} at room temperature using the equation reported previously,[8] which is smaller than that reported by Willner and coworkers (700 s^{-1}),[45] but higher than that using molecular wire as electrical communication between the active centre of GOx and the underlying GC electrodes.[8]

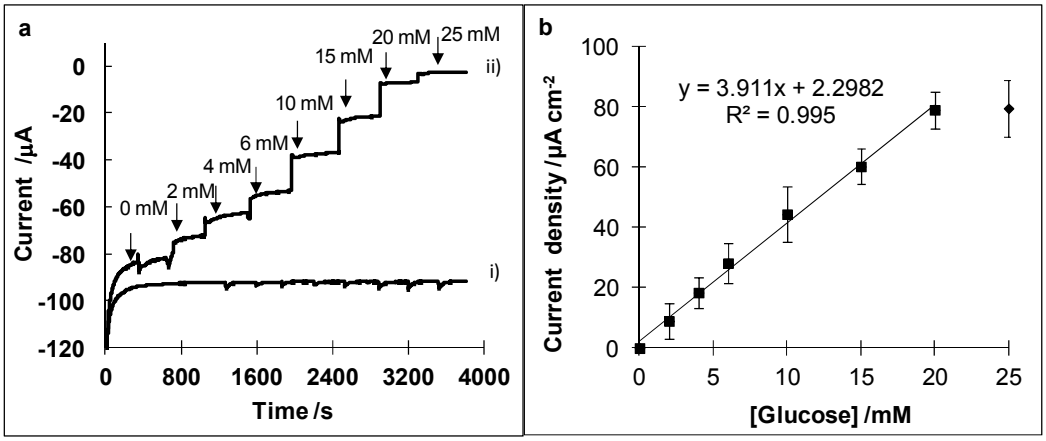

Figure 5. (a) The current record as a function of time for ii) GC/GO-Ph-AuNP-CP/GOx and i) GC/GO-Ph-AuNP-CP electrodes in 0.05 M phosphate buffer (oxygen-free, 0.05 M KCl, pH 7.0) at a constant potential of -0.43 V after adding glucose at different concentrations. (b) The increase of the oxidation

current versus the concentration of the glucose injected into the electrochemical cell under anaerobic condition for GC/GO-Ph-AuNP-CP/GOx electrode at (a).

Selectivity, reproducibility, and stability of GC/GO-Ph-AuNP-CP/GOx electrode

Similar to sensitivity, the selectivity of a device is a key parameter in its practical applications. Commonly presented in physiological samples, the interference from electroactive compounds, such as L-ascorbic acid (AA), uric acid (UA), dopamine (DA), acetaminophen (AP), fructose, galactose, and lactose may cause errors in the determination of glucose. In the physiological condition, the level of glucose (3 - 8 mM) is much higher than that of these species (<0.5 mM). We recorded the amperometric responses of 10 mM glucose, 100 mM of AA, UA, DA, AP, fructose, galactose and lactose in homogeneously stirred PBS solution, as shown in Figure 6 a. It was found that GC/GO-Ph-AuNP-CP/GOx electrode provide remarkable responses only for glucose oxidation, and there is no obvious amperometric current response for interfering species as compared to glucose, suggesting high selectivity of the modified sensing interface. The reproducibility of six GC/GO-Ph-AuNP-CP/GOx electrodes was estimated by the response to 10 mM glucose at the potential of -0.43 V. The results reveal that the sensor has satisfied reproducibility with a mean change of the response current of 42 μA cm^{-2} and a relative standard deviation of 5.05%. The stability of the GC/GO-Ph-AuNP-CP/GOx electrode under storage conditions (PBS, pH 7.0, 4 °C) was investigated using the same PBS containing 10 mM glucose. After 10 days, the response current is still retained at 90.3% value of the initial response in continuous tests (Figure 6 b), suggesting that the glucose sensor has favorable

long-term stability. Good stability is attributed to the covalent bonding on the sensing interface and enzyme entrapped strongly on AuNPs that is stable in the neutral medium. And the result implies that the fabricated GC/GO-Ph-AuNP-CP/GOx sensing interface is compatible with the immobilized enzyme and is helpful to maintain the bioactivity of GOx.

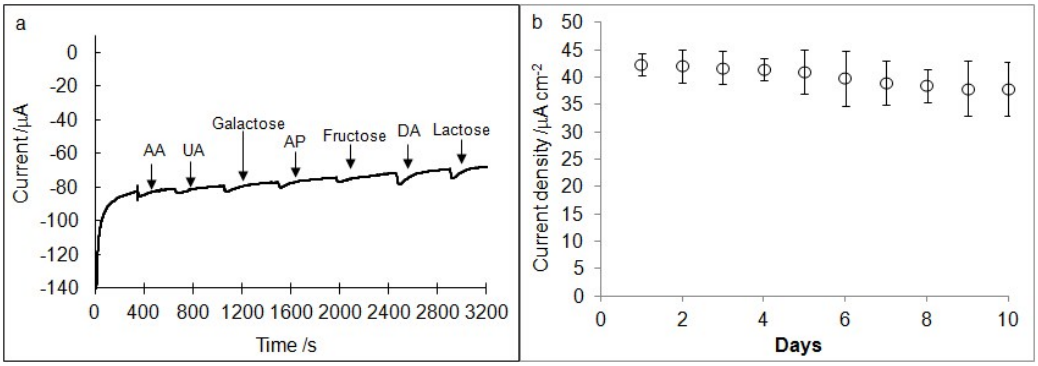

Figure 6. (a) The current record as a function of time for GC/GO-Ph-AuNP-CP/GOx electrodes in 0.05 M phosphate buffer (oxygen-free, 0.05 M KCl, pH 7.0) at a constant potential of -0.43 V after adding 100 mM of interference molecules. (b) The current density (recorded daily) of the GC/GO-Ph-AuNP-CP/GOx electrode after storing at PBS (pH 7.0, 4 °C) over 10 days.

Application of GC/GO-Ph-AuNP-CP/GOx sensing surface to monitor the consumption of glucose for HUVECs and HeLa cell lines

In this study, two cell lines (HUVECs and HeLa) were applied to test the glucose uptake rates by GC/GO-Ph-AuNP-CP/GOx sensing surface **(**Figure 7). Using the two hour time scale, the oxygen consumption and glucose uptake rates were calculated to be about 15.5 fmol·min^{-1}·cell^{-1} for HeLa cells and 8.8 fmol·min^{-1}·cell^{-1} for HUVECs cells. The glucose uptaking rate for HeLa cells is similar to that reported previously

(12.1 fmol·min^{-1}·cell^{-1}).[46]

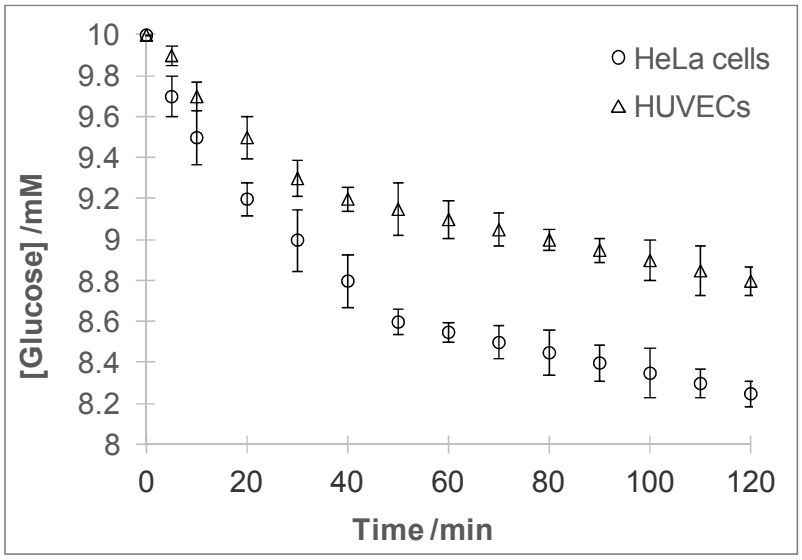

Figure 7. The glucose uptake assay by HUVECs and HeLa cells detected by the GC/GO-Ph-AuNP-CP/GOx sensing surfaces.

CONCLUSION

In this paper, we demonstrate a new method of prepare glucose biosensor based on gold nanoparticles loaded GO nanocomposites (GO-Ph-AuNP), which were prepared by integrating gold nanoparticles with GO via aryldiazonium salt reaction. The AuNP decoration was of even distribution on the GO, indicating that electrochemical reduction is an efficient method for the preparation of GO-Ph-AuNP nanocomposite. Then the glucose sensor was fabricated by modification of GO-Ph-AuNP to GC surface followed the attachment of 4-caboxyphenyl and GOx. GOx showed an enhanced direct electrochemistry on the nanocomposite modified electrode surface. The fabricated biosensor showed a good linear response toward glucose with the sensitivity of 42 μA mM^{-1} cm^{-2} and the enzyme turnover rate of 112 s^{-1} at room

temperature. The fast turnover rate observed in our system suggests that there is good electronic coupling between the redox active centre of GOx and the electrode. Thus it is promising for GO-Ph-AuNP nanocomposite to be be used an immobilization matrix for other redox active enzymes. Finally, GC/GO-Ph-AuNP-CP/GOx sensing surface has demonstrated the capability of simultaneously monitor in real-time the glucose consumptions by live cells.

ACKNOWLEDGEMENTS

This work was financially supported by the National Natural Science Foundation of China (Grant 21575045 and 31501566), the self-determined research funds of CCNU (CCNU15A02015), Scientific Research Foundation for the Returned Overseas Chinese Scholars from State Education Ministry and the funding from Macquarie University MQRDG and the ARC Centre of Excellence for Nanoscale Biophotonics CE140100003.

REFERENCES

(1) Aronoff, S. L.; Berkowitz, K.; Shreiner, B.; Want, L. *Diabetes Spectrum* **2004**, *17*, 183-190.
(2) Yun, J.; Rago, C.; Cheong, I.; Pagliarini, R.; Angenendt, P.; Rajagopalan, H.; Schmidt, K.; Willson, J. K.; Markowitz, S.; Zhou, S. *Science* **2009**, *325*, 1555-1559.
(3) Clark, L. C.; Lyons, C. *Annals of the New York Academy of sciences* **1962**, *102*, 29-45.
(4) Hsueh, C.-J.; Janyasupab, M.; Lee, Y.-H.; Liu, C.-C. In *Encyclopedia of Applied Electrochemistry*; Springer, 2014, pp 479-485.
(5) Steiner, M.-S.; Duerkop, A.; Wolfbeis, O. S. *Chemical Society Reviews* **2011**, *40*, 4805-4839.
(6) Li, S.; Davis, E. N.; Anderson, J.; Lin, Q.; Wang, Q. *Biomacromolecules* **2008**, *10*, 113-118.
(7) Ferri, S.; Kojima, K.; Sode, K. *Journal of diabetes science and technology* **2011**, *5*, 1068-1076.
(8) Liu, G.; Paddon-Row, M. N.; Gooding, J. J. *Electrochemistry Communications* **2007**, *9*, 2218-2223.
(9) Albers, W. M.; Lekkala, J. O.; Jeuken, L.; Canters, G. W.; Turner, A. P. *Bioelectrochemistry and bioenergetics* **1997**, *42*, 25-33.

(10) Conghaile, P. Ó.; Kamireddy, S.; MacAodha, D.; Kavanagh, P.; Leech, D. *Analytical and bioanalytical chemistry* **2013**, *405*, 3807-3812.
(11) Zhu, Z.; Garcia-Gancedo, L.; Flewitt, A. J.; Xie, H.; Moussy, F.; Milne, W. I. *Sensors* **2012**, *12*, 5996-6022.
(12) Yum, K.; McNicholas, T. P.; Mu, B.; Strano, M. S. *Journal of diabetes science and technology* **2013**, *7*, 72-87.
(13) Ahmad, M.; Pan, C.; Luo, Z.; Zhu, J. *The Journal of Physical Chemistry C* **2010**, *114*, 9308-9313.
(14) Courjean, O.; Gao, F.; Mano, N. *Angewandte Chemie International Edition* **2009**, *48*, 5897-5899.
(15) Allen, M. J.; Tung, V. C.; Kaner, R. B. *Chem. Rev.* **2010**, *110*, 132-145.
(16) Kannan, P. K.; Moshkalev, S. A.; Rout, C. S. *RSC Advances* **2016**.
(17) Liu, G. Z.; Zhang, Y.; Guo, W. *Biosens. Bioelectron.* **2014**, *61*, 547-553.
(18) Kannan, P. K.; Moshkalev, S. A.; Rout, C. S. *Nanotechnology* **2016**, *27*, 075504.
(19) Liu, J.; Fu, S.; Yuan, B.; Li, Y.; Deng, Z. *Journal of the American Chemical Society* **2010**, *132*, 7279-7281.
(20) Yin, P. T.; Shah, S.; Chhowalla, M.; Lee, K.-B. *Chemical reviews* **2015**, *115*, 2483-2531.
(21) Jasuja, K.; Berry, V. *Acs Nano* **2009**, *3*, 2358-2366.
(22) Kim, T.-H.; Lee, K.-B.; Choi, J.-W. *Biomaterials* **2013**, *34*, 8660-8670.
(23) Chuang, M.-K.; Lin, S.-W.; Chen, F.-C.; Chu, C.-W.; Hsu, C.-S. *Nanoscale* **2014**, *6*, 1573-1579.
(24) Chuang, M.-K.; Chen, F.-C.; Hsu, C.-S. *Journal of Nanomaterials* **2014**, *2014*.
(25) Fraser, S.; Zheng, X.; Qiu, L.; Li, D.; Jia, B. *Applied Physics Letters* **2015**, *107*, 031112.
(26) Liu, G. Z.; Qi, M.; Zhang, Y.; Cao, C. M.; Goldys, E. M. *Anal. Chim. Acta* **2016,** 909, 1-8.
(27) Bei, F.; Hou, X.; Chang, S. L.; Simon, G. P.; Li, D. *Chemistry-A European Journal* **2011**, *17*, 5958-5964.
(28) Huang, R.-C.; Chiu, W.-J.; Lai, I. P.-J.; Huang, C.-C. *Scientific reports* **2015**, *5*.
(29) Lingappan, N.; Kim, J. H.; Gal, Y. S.; Lim, K. T. *Molecular Crystals and Liquid Crystals* **2014**, *602*, 126-133.
(30) Shervedani, R. K.; Amini, A.; Sadeghi, N. *Biosensors and Bioelectronics* **2016**, *77*, 478-485.
(31) Liu, G. Z.; Luais, E.; Gooding, J. J. *Langmuir* **2011**, *27*, 4176-4183.
(32) Liu, G. Z.; Liu, J.; Böcking, T.; Eggers, P. K.; Gooding, J. J. *Chem. Phys.* **2005**, *319*, 136-146.
(33) Kraatz, H. B. *J. Organomet. Chem.* **1999**, *579*, 222-226.
(34) Sharma, P.; Darabdhara, G.; Reddy, T.M.; Borah, A. *Catal. Commun*. **2013**，*40*,139 – 144
(35) Yu, X.; Huo, Y.; Yang, J.; Chang, S. *Appl. Surf. Sci*. **2013**, *280* , 450– 455
(36) Akhavan, O.; Ghaderi, E. *Small* **2013**, *9*, 3593-3601.
(37) Abdelhalim, M. A. K.; Mady, M. M.; Ghannam, M. M. *Journal of Nanomedicine & Nanotechnology* **2012**, *2012*.

(38) Liu, G. Z.; Zhang, Y.; Guo, W. Q. *Biosens. Bioelectron.* **2014**, *61*, 547-553.
(39) Palanisamy, S.; Karuppiah, C.; Chen, S.-M. *Colloids and Surfaces B: Biointerfaces* **2014**, *114*, 164-169.
(40) Bourdillon, C.; Demaille, C.; Gueris, J.; Moiroux, J.; Saveant, J.-M. *J. Am. Chem. Soc.* **1993**, *115*, 12264-12269.
(41) Laviron, E. *J. Electroanal. Chem.* **1979**, *101*, 19-28.
(42) Yi, X.; Patolsky, F.; Katz, E.; Hainfeld, J.F.; Willner, I. Science 2003, 299, 1877–1881.
(43) Ravenna, Y.; Xia, L.; Gun, J.; Mikhaylov, A. A.; Medvedev, A. G.; Lev, O.; Alfonta, L. *Analytical chemistry* **2015**, *87*, 9567-9571.
(44) Wu, P.; Shao, Q.; Hu, Y.; Jin, J.; Yin, Y.; Zhang, H.; Cai, C. *Electrochimica Acta* **2010**, *55*, 8606-8614.
(45) Zayats, M.; Katz, E.; Willner, I. *J. Am. Chem. Soc.* **2002**, *124*, 2120-2121.
(46) Zhang, L.; Su, F.; Buizer, S.; Lu, H.; Gao, W.; Tian, Y.; Meldrum, D. *Biomaterials* **2013**, *34*, 9779-9788.